Uncooled rectifying and resistive type sub-THz direct detection detectors. Upper limit performance

F. Sizov, A. Golenkov, M. Sakhno, V. Zabudsky, Z. Tsybrii
Lashkaryov ISP of Ukrainian NAS,
Kiev, Ukraine
sizov@isp.kiev.ua

S. Dvoretskii, N. Mikhailov
Rzhanov ISP of SB RAS
Novosibirsk, Russia
dvor@isp.nsc.ru

Abstract— **Performance of terahertz THz field effect transistor (FET) direct detection rectifying detectors operating in the broadband detection regime taking into account some extrinsic parasitics and detector-antenna impedance matching is considered. *Si* metal oxide semiconductor FET (MOSFET) and *GaAlN/GaN* heterojunction FET (HFET) THz detectors in comparison with Schottky barrier diode (SBD) ones are discussed. Optical responsivity $\Re_{opt}$ and optical noise equivalent power NEP_{opt} were estimated. The mercury-cadmium-telluride (MCT) hot electron bolometers (HEBs) as THz detectors also were considered.**

Keywords — THz detectors; field-effect transistors; NEP_{opt}.

I. INTRODUCTION

Terahertz (THz) technologies ($\nu \sim 0.1\ldots10$ THz) have potential applications in vision systems, high speed wireless communications, pharmacology, environmental control, as well as security and quality-control applications [1,2]. Along with the sources the important components of these technologies are uncooled detectors.

Si MOSFET, *III-V* heterojunction FET (HFET) and *III-V* Schottky barrier diode (SBD) rectification detectors now are among the promising THz/sub-THz direct detection detectors. The uncooled SBD single detectors at the moment are the most sensitive ones especially at low frequency THz range (<~100 GHz) where their $NEP_{opt} \sim 10^{-12}\ldots4\cdot10^{-13}$ W/Hz$^{1/2}$. The study of FET THz detectors was initiated by Dyakonov-Shur [3] publication though images by small number *GaAs* FET arrays were demonstraited earlier [4]. To the moment FET detectors also have rather appropriate responsivity characteristics ($NEP_{opt} \sim 10^{-10}\ldots10^{-11}$ W/Hz$^{1/2}$ in dependence of technology design rules and radiation frequency ν regions).

All these detectors are rather fast ($\tau \sim 10^{-9}$ s, *Si* MOSFETs [5], $\tau \sim 10^{-11}$ s, *GaAs* FETs [6], $\tau \sim 10^{-11}$ s, SBDs [7]). As direct detection detectors they can operate in wide spectral ranges (for *Si* MOSFET detectors $\nu \leq 9$ THz [5], for SBDs $\nu \leq 10$ THz [8]. The important task for application of these detectors e.g. in direct detection vision systems is the estimation of their performance ($\Re_{opt}$ and NEP_{opt}) at least taking into account their basic extrinsic parasitics and the detector-antenna coupling.

FET and HFET detectors are the direct detection rectifying detectors with broadband (non-resonant) detection when their channel length L is larger the short channel distance near the source L_{eff}. Within $L_{eff} = \sqrt{\frac{\sigma_{CH} \cdot L^2}{\omega \cdot C_{CH}}}$ the rectification occurs, and it is of the order of a few tens nm [9]. Here $\sigma_{CH} = \left.\frac{\partial I_{DS}}{\partial V_{DS}}\right|_{V_{DS}=0V}$ is the channel conductivity, I_{DS} is the drain-source current and C_{CH} is the channel capacity, $\omega = 2\pi\nu$, ν is the radiation frequency.

II. CURRENTS AND VOLTAGES

For rectifying detectors an important issue to get NEP_{opt} values is the necessity of accounting of the impedances of the antenna Z_A and that of the device Z_{det} with the extrinsic parasitic X_P, R_S (see Fig. 1)

$$Z_{det} = R_S + \frac{X_P(\omega) \cdot Z_{INT}(x,\omega)}{X_P(\omega) + Z_{INT}(x,\omega)}, \quad (1)$$

where R_S and $X_P = -j/(\omega \cdot C_P)$ are the parasitic serial resistance and parasitic component connected with the parasitic shunting capacity C_P, respectively, $j=(-1)^{1/2}$, the parameter $x = \frac{V_{GS} - V_{TH}}{n \cdot \varphi_t}$ or $x = \frac{V_D}{n \cdot \varphi_t}$ for FET (HFET) and SBD detectors, respectively, $\varphi_t = k_B \cdot T/q$ is the thermal potential, V_{TH} is the threshold voltage, V_{GS} is the gate-source voltage, V_D is the SBD voltage and the $n \sim 1\ldots10$ (ideality factor for SBDs or slope of curve for FETs, typically $n \sim 1.1\ldots1.3$ for SBDs, $n \sim 1.3\ldots1.5$ for *Si* MOSFETs; $n \sim 10$ [10] for *GaAlN* HFETs for room temperature conditions), $Z_{INT} = Z_{GS,int}$ where $Z_{GS,int}$ is the internal source-gate impedance, C_p is the parasitic shunting capacity. In Fig. 1 by ΔV_0 is indicated the signal amplitude. The parameters X_P, Z_A and Z_{int} are dependent on ν.

978-1-4673-7434-7/15/$31.00 ©2015 IEEE
This work is supported by NATO Project SfP 984544.

In publications (see e.g. [3,10-12]) the attention primarily was concentrated on the electrical $\Re_{el}$ responsivity or electrical NEP_{el} rather than on the optical NEP_{opt}. The latter one takes into account the antenna properties, its matching efficiency with the detector and matching with the measuring facility.

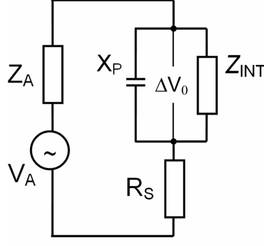

Fig. 1. Simplified schematic representation of rectifying THz detector taking into account the basic extrinsic parasitic components.

Under the THz radiation with frequency ω and arising high frequency voltage signal between the FET source and gate $\Delta V_0 \cdot \sin(\omega \cdot t)$ (when antenna is connected between the source and gate) the detector rectified current δI_{det}

$$\delta I_{\det} = \frac{\Delta V_0^2}{4} \cdot \frac{1}{n \cdot \varphi_t} \cdot \sigma_0 \cdot \frac{\partial f_\sigma(x)}{\partial x}(2-n) \cdot \qquad (2)$$

For SBDs with zero bias ($V_D = 0$) the parameter $\sigma_0 = \sigma_{0,SBD} = I_0/n\cdot\varphi_t$ is the differential conductivity of the metal-semiconductor contact and the dimensionless parameter

$$f_\sigma(x) = \frac{df_D(x)}{dx} = e^x \cdot \qquad (3)$$

For FETs (HFETs) $\sigma_0 = I_0/\varphi_t$ is the coefficient that characterizes the channel conductivity and $f_\sigma(x)$ is the dimensionless parameter that takes into account the conductivity changes on the gate-source voltage V_{GS}

$$f_\sigma(x) = \frac{\partial f_{DS}(x,0)}{\partial y} = \frac{2 \cdot \ln(1+e^{\frac{x}{2}}) \cdot e^{\frac{x}{2}}}{(1+e^{\frac{x}{2}})} \,. \qquad (4)$$

The detector voltage is

$$\delta V_{\det} = \frac{\delta I_{\det}}{\sigma_0 \cdot f_\sigma(x)} \cdot \eta_L(x) \cdot \qquad (5)$$

The coefficient η_L takes into account the voltage divider between the detector resistance and the load impedance Z_L of the registration system.

THz radiation through the antenna generate in the antenna-detector circuit the high frequency voltage with the amplitude V_A which than is transferred and rectified at the metal-semiconductor interface in SBDs or at the $\sim L_{eff}$ in FETs.

In SBDs the internal impedance is the differential resistance of the metal-semiconductor contact [13] $Z_{int} = 1/\sigma_0$. In FETs the internal impedance can be calculated for double-pass line with distributed parameters [14]

$$Z_{\text{int}}(x,\omega) = Z_{SG,\text{int}}(x,\omega) = \sqrt{\frac{1}{2 \cdot \sigma_{CH}(x) \cdot \omega \cdot C_{CH}}} \cdot (1-j) \,, \qquad (6)$$

where $\sigma_{CH} = \sigma_0 \cdot f_\sigma(x)$, $C_{CH} \approx W \cdot L \cdot C_{ox}^{/}$ (in the strong inversion regime approximation) are the channel conductivity and capacity of FET channel, respectively.

Taking into account the circuit in Fig. 1

$$\Delta V_0^2(x) = \xi_Z(x) \cdot V_A^2 = \left| \frac{X_P \,\|\, Z_{\text{int}}(x)}{Z_A + R_S + X_P \,\|\, Z_{\text{int}}(x)} \right|^2 \cdot V_A^2 \,, \qquad (7)$$

where ξ_Z is the transfer coefficient of square voltage from the antenna to transistor.

The antenna impedance can be written as [15]

$$Z_A = R_A + j \cdot X_A = R_{A,R} + R_{A,L} + j \cdot X_A \,, \qquad (8)$$

where R_A and X_A are the real and imaginary parts, respectively, $R_{A,R}$ is the radiation antenna resistance, and $R_{A,L}$ is the resistance of losses. The antenna voltage V_A is

$$V_A = E_{THz} \cdot l_A = E_{THz} \cdot \lambda \cdot \sqrt{\frac{R_{A,R} \cdot D_0}{\pi \cdot Z_0}} \,, \qquad (9)$$

where E_{THz} is the field strength,

$$l_A = \lambda \cdot \sqrt{\frac{R_{A,R} \cdot D_0}{\pi \cdot Z_0}} \qquad (10)$$

is the antenna dipole effective length [16], $Z_0 \approx 377\,\Omega$ is the free-space impedance, λ is the radiation free-space wavelength, D_0 is the antenna directivity coefficient.

The radiation power P_{opt} falling down on the detector physical area A_{opt}

$$P_{opt} = W_{THz} \cdot A_{opt} = \frac{E_{THz}^2}{2 \cdot Z_0} \cdot A_{opt} = \frac{V_A^2}{8 \cdot R_{A,R}} \cdot \frac{4\pi \cdot A_{opt}}{\lambda^2 \cdot D_0} \,, \qquad (11)$$

where W_{THz} is the power density of the e.m. wave. Finally for current optical responsivity $\Re_{I,opt} = \delta I_{det}/P_{opt}$ it follows for SBD and FET type detectors

$$\Re_{I,opt} = \frac{2 \cdot R_{A,R} \cdot \sigma_0}{\varphi_t} \cdot \left| \frac{2-n}{n} \right| \cdot f_\sigma^{'} \cdot \xi_Z \cdot \xi_{opt} \cdot D_0 \,, \qquad (12)$$

and for voltage responsivity $\Re_{V,opt} = \delta V_{det}/P_{opt}$

$$\Re_{V,opt} = \frac{2 \cdot R_{A,R}}{\varphi_t} \cdot \left| \frac{2-n}{n} \right| \cdot \frac{f_\sigma^{'}}{f_\sigma} \cdot \eta_L \cdot \xi_Z \cdot \xi_{opt} \cdot D_0 \,, \qquad (13)$$

where the coefficient $\xi_{opt} = \dfrac{\lambda^2}{4\pi \cdot A_{opt}}$ characterizes the efficiency of antenna and $f_\sigma^{'} = df_\sigma / dx$.

The optical $NEP_{opt} = V_{noise}/\Re_{V,opt}$ expression for minimal noise which is the Johnson-Nyiquist noise [17,18] in FETs at zero bias V_{DS} and SBDs at $V_D = 0$

$$V_{noise} = \sqrt{4 \cdot k_B \cdot T \cdot (r_{dsw} \cdot W^{-1} + R_0 \cdot f_\sigma^{-1})} = 2 \cdot q^{1/2} \cdot \varphi_t^{1/2} \cdot (r_{dsw} \cdot W^{-1} + R_0 \cdot f_\sigma^{-1})^{1/2} \qquad (14)$$

and

$$NEP_{opt} = \frac{q^{1/2} \cdot \varphi_t^{3/2} \cdot R_0^{1/2}}{R_{A,R}} \cdot \left| \frac{n}{2-n} \right| \cdot \left(\frac{r_{dsw}}{R_0 \cdot W} + \frac{1}{f_\sigma} \right)^{1/2} \times \frac{f_\sigma}{f_\sigma^{'}} \cdot \frac{1}{\xi_Z \cdot \xi_{opt} \cdot D_0} \,. \qquad (15)$$

Exps. (12), (13), (15) are valid for MOSFET detectors. For

HFET detectors they were taken as similar ones because of there is absent the appropriate treatment of their properties.

The resistance $R_0 = 1/\sigma_0$ and the parameter r_{dsw} is the resistance per unit transistor width between the source and drain areas (except channel resistance), Ω·μm. r_{dsw} can be taken from BSIM3.3, BSIM4 models or from *I-V* transistor

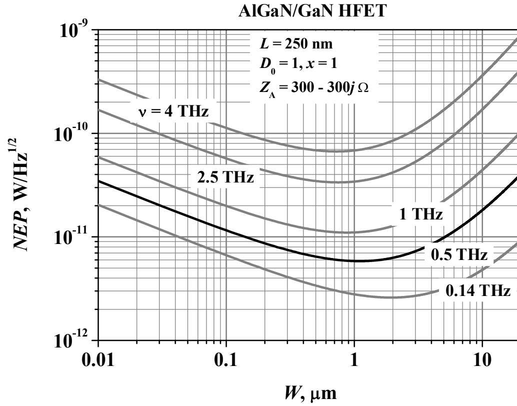

Fig. 2. NEP_{opt} of *GaAlN/GaN* HFETs in function of channel width W with channel length L=0.25 μm. T=300 K, n=1.3, Z_A= 100 - 100·j Ω. For optimal NEP_{opt} $x \sim 1$.

characteristics. This coefficient can play a substantial role in devices with high electron mobility. In *Si* FETs its influence is less notable as the channel resistance influence is much more important. For SBDs the coefficient $r_{dsw} = 0$. The parameter η_L depends on the registration setup and for estimations it was taken $\eta_L = 1$. The minimum value of the function $f_\sigma^{1/2} / f_\sigma^{'} \approx 1.75$ and the maximum value of the function $f_\sigma^{'} / f_\sigma = 1$ defines the optimum NEP_{opt} and sensitivity $\Re_{V,opt}$ values, respectively. For SBD detectors the parameter $|n/(2-n)|$ must be changed to n, the values $f_\sigma = f_\sigma^{1/2} = f_\sigma^{'} = 1$. The ultimate NEP_{opt} value of MOSFET detectors is worse by a factor 1.75 compared to SBD ones (not taking into account the differences in frequency dependences of the antenna properties and those of the devices).

The ultimate value $NEP_{opt} \sim 10^{-12}$ W/Hz$^{1/2}$ for MOSFET detectors follows from Eq. (15) under the assumptions $n = 1$, $R_{A,R}$= 300 Ω, T = 300 K, $R_0 = 10^4$ Ω, $\xi_Z = \xi_{opt} = D_0 = 1$, $r_{dsw} = 0$ Ω·μm. Coefficient ξ_Z is dependent on the mismatch antenna-detector impedances and can be improved by introducing some compensating elements in detector reactive component to increase the power losses at the detector active element. Coefficient ξ_{opt} can be larger or less compared to 1 and is dependent on detector and antenna design. Directivity D_0 can be >> 1 but for vision systems with relatively large arrays it should be ~1.0...1.5.

One of the important FET (HFET) parameters is the channel resistance $R_0 = L/(W \cdot \mu_n \cdot C_{ox}^{'} \cdot n \cdot \varphi_t)$ [19] which is in direct proportion to the channel length L, and inversely proportional to the channel width W and mobility μ_n. To reduce R_0 (e.g. for reducing Johnson-Nyiquist noise) the length L is designed as small as manufacturing design rules allow. But the width W can be optimized to get better NEP_{opt} performance. To decrease the resistance R_0 the width W should be increased. At the same time, the width W cannot be very wide as the gate parasitic serial resistance R_S becomes large [14]

$$R_S = r_0 + r_1 / W + r_2 \cdot W / (3 \cdot L)\,, \qquad (15)$$

where r_0 is the resistance of the contacts between the metal and gate layers (~5 Ω), r_1 is the transistor source resistivity (r_1=r_{dsw}/2) and r_2 is the gate material resistivity. For *III-V* HFETs (e.g. *AlGaN/GaN*) in which the gate has a Schottky barrier, the metallic gate resistivity r_2 is considerably smaller than the polysilicon one in *Si* MOSFETs.

Typically in *Si* MOSFETs r_1 and r_2 values are $r_1 \sim 400$ Ω·μm, $r_2 \sim 40$ Ω (in the 0.35 μm technology design rules, as for example), and in the *AlGaN/GaN* HFETs the value $r_2 < 0.1$ Ω. To avoid power losses the value of R_S have to be smaller the antenna radiation resistance $R_{A,R}$ ($R_{A,R}$ ~100…300 Ω in dependence of the antenna type [5]).

The width W also is limited by parasitic shunting capacitance X_P between the transistor gate and source. It is dependent on radiation frequency ν, shunting capacity C'_P per unit width (is equal to *cgdo* or *cgso* parameters in BSIM3.3, BSIM4 models), and the channel width W [14]

$$X_P = -j / (2 \cdot \pi \cdot \nu \cdot W \cdot C_P^{'})\,. \qquad (16)$$

The $C_P^{'}$ values depend on design rules technology (e.g. $C_P^{'} \approx 2 \cdot 10^{-10}$ F/m for 0.35 μm *Si* MOSFET design rules). It is assumed that the influence of the channel width W on capacitance X_P for *AlGaN/GaN* HFETs and *Si* MOSFETs are similar in the character.

In Fig. 2 as for example are presented the calculated NEP_{opt} dependencies for *GaAlN/GaN* HFET direct detection detectors on channel width W for different radiation frequencies ν. One can note the strong dependences of the optimal NEP_{opt} at different radiation frequencies on channel width. The minimum NEP_{opt} is shifting with ν growth to shorter W. For *Si* FETs the dependences are rather similar but W values are shifted to lower values.

In Fig. 3 are presented the calculated and some experimental values of NEP_{opt} for Si MOSFET detectors.

For comparison MCT thin layers also were considered as uncooled HEB THz detectors. The responsivity mechanisms in such detectors for the case of intrinsic conductivity are different compared to the well known low-temperature nature of the response connected with electron gas heating. The particles motion in intrinsic MCT detectors under the THz radiation is governed by the three different contributions, which can lead to positive or negative THz photoconductivity. These contributions are: (i) the Dember effect (photo-diffusion effect) contribution, (ii) the thermo-electromotive contribution, and (iii) the contribution associated with changes of free carrier concentration.

The response of MCT THz bolometers (τ <~ 10^{-7} s) was measured at ν = 0.037-1.54 THz and T = 68-300 K. MCT detectors with antennas were also considered as two-colour

uncooled sub-THz ($\nu \approx 140$ GHz) direct detection bolometers and 3...10 μm infrared (IR) photoconductors. *NEP* for sub-THz detectors studied at $\nu \approx 140$ GHz reaches $NEP_{opt300K} \approx (2.5 - 4.5 \cdot 10^{-10})$ W/Hz$^{1/2}$. The same detectors used as IR photoconductors showed reasonable responsivity at 300 K to be used in some applications. To acquire THz images common experimental layout based on irradiation transmission or reflection of objects and two-coordinate mechanical scanning were used.

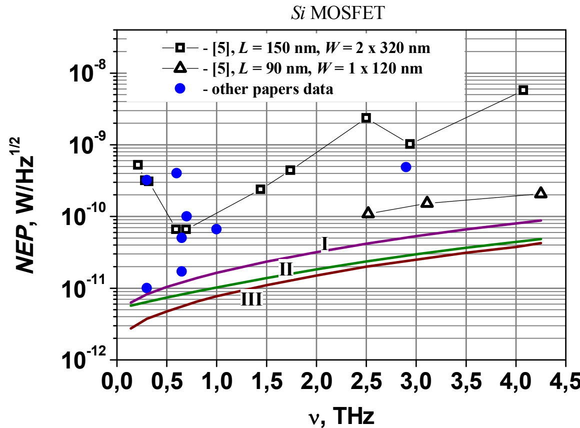

Fig. 3. Experimental values of NEP_{opt} from [5] for *Si* FETs were recalculated for antenna area $\lambda^2/4\pi$ instead of physical area of the patch antennas used in [5] (antenna impedance $Z_A = 300...300 \cdot j\ \Omega$). Calculated curves ($L$ = 90 nm, D_0 =1): I is for the optimal width W, $Z_A = 100 - 100j\ \Omega$; II is for W = 1x120 nm, $Z_A = 300 - 300j\ \Omega$; III is for the optimal width W, $Z_A = 300 - 300j\ \Omega$. Data from other papers were represented as they are and were taken from References cited in [14]. Calculations were done for optimal *W*.

From the analysis above it can be concluded that uncooled rectifying and narrow-gap MCT bolometer type THz detectors can only be applied in active direct detection vision systems.

III. Conclusions

Optical responsivity $\Re_{opt}$ and noise equivalent power NEP_{opt} of unbiased (zero drain-source bias V_{DS} = 0) FETs, HFETs and SBDs (bias V_D = 0) as THz/sub-THz detectors were considered. Taking into account some basic extrinsic parasitics and detector-antenna impedance matching it is possible to estimate FET detectors ultimate performance limits choosing the appropriate channel width W at certain radiation frequency ν. The estimated ultimate NEP_{opt} value of FET detectors is worse by factor ~1.75 compared to SBDs (not taking into account the differences in frequency dependences of the antenna properties and those of the devices under consideration).

Uncooled MCT HEB detectors show worse characteristics compared to rectifying THz detectors but can operate both in THz and IR spectral ranges. Uncooled rectifying and narrow-gap MCT bolometer type THz detectors can only be applied in active direct detection vision systems.

IV. References

1. D. Saeedkia (ed.), *Handbook of terahertz technology for imaging, sensing and communications*, Woodhead Publishing Limited, Oxford Cambridge Philadelphia New Delhi, 2013, pp. 1-678.
2. Kai-Erik Peiponen, J. Axel Zeitler and Makoto Kuwata-Gonokami (eds.), *Terahertz Spectroscopy and Imaging*. Springer Series in optical Sciences, vol. 171, Heidelberg-New York-Dordrecht-London, 2013, pp. 1–641.
3. M. Dyakonov, and M. Shur, Plasma wave electronics: Novel terahertz devices using two dimensional electron fluid, *IEEE Trans. Electron Devices*, **43**, 1640-1645 (1996).
4. W. Chew and H. R. Fretterman, Millimeter-wave imaging using FET detectors integrated with printed circuit antennas, *Int. J. Infr. Milli. Waves*, **10**, 565-578 (1989).
5. A. Lisauskas, M. Bauer, S. Boppel, M. Mundt, B. Khamaisi, E. Socher, R. Venckevicius, L. Minkevicius, I. Kasalynas. D. Seliuta, G. Valusis, V. Krozer, and H. G. Roskos, Exploration of terahertz imaging with silicon MOSFETs, *J Infrared Milli Terahz Waves*, **35**, 63–80 (2014).
6. S. Preu, M. Mittendorf, S. Winnerl, H. Lu, A.C. Gossard, and H.B. Weber, *Opt. Express*, 21 (15), 17941 - 17950 (2013).
7. L. Liu, J.L. Hesler, H. Xu, A.W. Lichtenberger, and R.M. Weikle, A Broadband Quasi-Optical THz Detector Using a Zero Bias Schottky Diode, *IEEE Microwave and Wireless Components Letters*, **20**, 504 (2010).
8. A. J. M. Kreisler, Submillimeter wave applications of submicron Schottky diodes, *Proc. SPIE*, **666**, 51 - 63 (1986).
9. W. Knap and M. Dyakonov, *Field effect transistors for terahertz applications*, in Handbook of Terahertz Technology, ed. by D. Saeedkia (Woodhead Publishing, Waterloo, Canada, 2013), pp. 121–155.
10. W. Knap, V. Kachorovskii, Y. Deng, S. Rumyantsev, J.-O. Lu, R. Gaska, M.S. Shur, G. Simin, X. Hu, M.A. Khan, C.A. Saylor, and L.C. Brunel, Nonresonant detection of terahertz radiation in field effect transistors, *J. Appl. Phys*., **91**, 9346 - 9353 (2002).
11. V. Yu. Kachorovskii, S. L. Rumyantsev, W. Knap, and M. Shur, Performance limits for field effect transistors as terahertz detectors, *Appl. Phys. Lett*., **102**, 223505 (2013).
12. E. Öjefors, A. Lisauskas, D. Glaab, H. G. Roskos, and U. R. Pfeiffer Terahertz imaging detectors in CMOS Technology, J Infrared Milli Terahz Waves, **30**, 1269-1280 (2009).
13. A. M. Cowley and Sorensen, Quantitative comparison of solid-state microwave detectors, *IEEE Transactions on Microwave Theory and Techniques*, **14**, 588 - 602 (1966).
14. M. Sakhno, A. Golenkov and F. Sizov, Uncooled detector challenges: Millimeter-wave and terahertz long channel field effect transistor and Schottky barrier diode detectors, *J Appl. Phys*., **114**, 164503 (2013).
15. C. A. Balanis, *Antenna Theory Analysis and Design*, Third Edition, Wiley, New Jersey (2005).
16. J. L. Volakis (ed.), *Antenna Engineering Handbook* (4th Ed.), New York, McGraw-Hill (2007).
17. R. Tauk, F. Teppe, S. Boubanga, D. Coquillat, W. Knap, Y.M. Meziani, C. Gallon, F. Boeuf. T. Scotnicki, C. Fenouillet-Beranger, D.K. Maude, S. Rumyantsev, and M.S. Shur, Plasma wave detection of terahertz radiation by silicon field effects transistoprs: Responsivity and noise equivalent power, *Appl. Phys. Lett*., **89**, 253511 (2006).
18. A. Lisauskas, S. Boppel, J. Matukas, V. Palenskis, L. Minkevicius, G. Valusis, P. Haring-Bolıvar, and H. G. Roskos, Terahertz responsivity and low-frequency noise in biased silicon field-effect transistors, *Appl. Phys. Lett*., **102**, 153505 (2013).
19. Y. Tsividis and C. McAndrew, *Operation and Modeling of the MOS Transistor*, Oxford University Press (2011).
20. M. S. Shur and P. Maki (eds.), Advanced High Speed Devices," in: *Selected Topics in Electronics and Systems*, vol. 51, World Scientific, Singapore, 2009.